nature communications

Article

https://doi.org/10.1038/s41467-025-65407-6

Desat1-mediated lipid homeostasis mitigates 20E-induced lipotoxicity in blood-fed mosquitoes

Received: 11 May 2025

Accepted: 14 October 2025

Published online: 25 November 2025

Check for updates

Peilu Sun[1,2,4], Guandong Wang[1,2,4], Bingchen Yang[1,2], Yiguan Wang[1,2], Chunlai Cui[1,2,3], Ling Dong[1,2], Yifei Li[1,2], Tao Zhou[1,2], Fang Li[1,2] & Sibao Wang[1,2]

Adequate lipid storage capacity is crucial for animal reproductive success, especially in female mosquitoes, which must accumulate sufficient lipid reserves to support egg production. However, the molecular mechanisms regulating lipid accumulation and the consequences of inadequate lipid stores remain poorly understood. Here, we show that *stearoyl-CoA desaturase 1* (*desat1*) is indispensable for lipid reserve establishment and metabolic balance in female *Anopheles* and *Aedes* mosquitoes. Knockdown of *desat1* of newly emerged females results in high mortality following a blood meal, whereas silencing *desat1* of older mosquitoes does not affect survival. Moreover, *desat1* activity of early-emerged females is essential for egg production and peritrophic matrix integrity. Lipidomic analyses reveal that silencing *desat1* impairs the conversion of saturated fatty acids (SFAs) to unsaturated fatty acids (USFAs), disrupting triglyceride synthesis and leading to SFA accumulation. After blood feeding, accumulated SFAs induce lipotoxicity, characterized by elevated oxidative stress and apoptosis. We further find that blood meal-derived proteins stimulate the 20-hydroxyecdysone (20E) signaling pathway, thereby exacerbating fatty acid β-oxidation, increasing reactive oxygen species (ROS) production, and inducing extensive apoptotic cell death in *desat1*-silenced early-emerged females, ultimately leading to mortality. Our findings reveal Desat1 as a critical metabolic safeguard against hormone-induced lipotoxicity in blood-feeding insects, establishing a novel mechanistic link between classical lipid metabolism and steroid hormone signaling, and identifying *desat1* as a promising target for vector control strategies.

Animals must accumulate adequate energy storage to support reproduction and ensure species survival. In the typical mode of reproduction involving yolk-containing eggs, female insects accumulate large amounts of energy reserves to support egg production[1]. Triglyceride (TAG), the primary long-term lipid energy storage, consists of three fatty acid chains esterified to a glycerol backbone[2]. On account of its higher C–H bond content compared to polysaccharides, TAG is an efficient energy reservoir[3,4]. It is well established that lipid reserves rapidly accumulate after adult eclosion of hematophagous disease-transmitting arthropods[5]. Despite the importance of lipid storage in

[1]New Cornerstone Science Laboratory, Key Laboratory of Insect Developmental and Evolutionary Biology, State Key Laboratory of Plant Trait Design, CAS Center for Excellence in Molecular Plant Sciences, Institute of Plant Physiology and Ecology, Chinese Academy of Sciences, Shanghai, China. [2]CAS Center for Excellence in Biotic Interactions, University of Chinese Academy of Sciences, Beijing, China. [3]Shanghai Institute of Wildlife Epidemics, School of Life Sciences, East China Normal University, Shanghai, China. [4]These authors contributed equally: Peilu Sun, Guandong Wang. e-mail: sbwang@cemps.ac.cn

reproduction, the mechanisms regulating lipid accumulation and the pathophysiological consequences of inadequate lipid stores in relation to reproduction remain understudied.

Anopheles mosquitoes are the vectors of human malaria, a leading cause of global morbidity and mortality[6,7]. The recent introduction and rapid expansion of the *Anopheles stephensi* mosquito in Africa poses a significant challenge to malaria control efforts and public health[8]. As such, a better understanding of mosquito physiology is paramount for developing innovative mosquito control strategies. After eclosion, female mosquitoes initially feed on plant nectar that sustains basic physiological functions and is converted into lipid reserves, primarily in the form of TAG[9]. However, nectar-derived lipid reserves alone are insufficient to meet the substantial energetic requirements for reproduction, necessitating a blood meal to support egg development[10]. Blood digestion also promotes the proliferation of gut microbiota, eliciting immune responses to control bacterial over-proliferation and to maintain intestinal homeostasis[11]. Both reproduction and immune responses are energetically demanding processes that rely on the mobilization of stored lipids[12], emphasizing the importance of lipid metabolism and homeostasis in mosquito biology.

Unsaturated fatty acids (USFAs) are required for maintaining proper lipid metabolism[13]. TAG, synthesized from USFAs and glycerol, serves as vital lipid reserves stored primarily in the insect fat body[14]. In mammals, imbalanced or insufficient USFAs intake is associated with metabolic diseases such as obesity, diabetes, inflammation, and cancer[13,15]. USFAs are produced via Δ9-cis desaturation of saturated fatty acyl-CoAs, catalyzed by the rate-limiting enzyme stearoyl-CoA desaturase 1 (Desat1), with palmitoyl- and stearoyl-CoA as preferred substrates[16]. In mice, knockdown of *desat1* diminishes lipogenesis and exacerbates metabolic pathologies[17]. In insects, studies of *desat1* have primarily focused on its role of cuticular hydrocarbons (CHCs) synthesis and of pheromone production for chemical communication[18–20]. Studies in the fruit fly *Drosophila melanogaster*[21] and the brown planthopper *Nilaparvata lugens*[22] showed that silencing *desat1* leads to stunted growth and shorter lifespan. Despite these insights, the mechanisms by which insects maintain balanced lipid metabolism and the specific role of *desat1* in this process remain unclear.

An. stephensi desat1 has been implicated in regulating heptacosane production, a male mating pheromone[19]. In this study, we show that *desat1* is crucial for post-blood feeding survival of newly emerged female mosquitoes, via regulation of lipid homeostasis. We found that silencing *desat1* disrupts lipid metabolism, decreases the unsaturated-to-saturated fatty acid (USFA/SFA) ratio, and induces lipotoxicity. We also show that in *desat1*-silenced mosquitoes, blood proteins activate the 20-hydroxyecdysone (20E) pathway, promoting fatty acid β-oxidation, which in turn leads to oxidative stress and apoptosis, ultimately leading to mosquito death.

Results

Silencing *desat1* of newly emerged females results in lethality and reduced fecundity following blood-feeding

Expression of the *An. stephensi desat1* gene (*ASTEO06887*, homologous to the *AGAP001713 An. gambiae* gene) is significantly higher in females compared to males (Supplementary Fig. 1a). Among female tissues, the fat body exhibited the highest *desat1* expression (Supplementary Fig. 1b), whereas *desat1* expression was low in eggs, larvae, and pupae (Supplementary Fig. 1a). Notably, *desat1* expression in the female fat body was low at eclosion, increased markedly to peak levels at 24 h after eclosion, and subsequently fluctuated (Supplementary Fig. 1c), These data suggest that *desat1* may play an important role during early post-eclosion development.

To investigate the functional role of *desat1* during post-eclosion (PE) times in female mosquitoes, we silenced *desat1* at early (18 h) and late (72 h) PE via injection of *desat1* double-stranded RNA (ds*desat1*) (Supplementary Fig. 2). For sugar-fed females, silencing *desat1* at 18 h PE resulted in significant mortality over a 15-day period ($p < 0.0001$), whereas silencing at 72 h PE did not significantly affect overall survival (Supplementary Fig. 3). To further assess the impact of *desat1* silencing, mosquitoes were provided with a blood meal 3 days after dsRNA injection (Fig. 1a). Surprisingly, mosquitoes silenced at 18 h PE exhibited a 71% mortality rate by three days post-blood meal (PBM) ($p < 0.0001$), whereas those silenced at 72 h PE were unaffected ($p > 0.05$) (Fig. 1b, c). However, ovarian development was severely impaired in both groups, with early-silenced females producing no eggs and late-silenced females laying markedly reduced eggs compared to controls (Fig. 1d, e). Collectively, these results indicate that *desat1* function during early post-eclosion stage is essential for post-blood feeding survival and normal vitellogenesis.

Silencing *desat1* in newly-emerged females promotes gut bacteria proliferation and prevents peritrophic matrix formation following a blood meal

Normally, following a blood meal, the blood bolus gradually darkens from light red to dark and decreases in size as digestion progresses. In contrast, *desat1*-silenced mosquitoes died shortly after feeding, retained an undigested bolus, and showed markedly delayed bolus darkening relative to dsGFP controls (Fig. 1f). Although expression of most trypsin genes was up-regulated (Supplementary Fig. 4a–e), enzymatic activity remained unchanged (Supplementary Fig. 4f). Therefore, failure of blood digestion in *desat1*-silenced mosquitoes does not appear to stem from insufficient trypsin activity.

A notable consequence of *desat1* knockdown was a marked increase in gut bacterial load (Fig. 1g). The peritrophic matrix (PM), produced by midgut epithelial cells (ECs) in response to blood feeding, serves as a physical barrier against invading pathogens and the over-proliferation of symbiotic bacteria[23]. Transmission electron microscopy (TEM) analysis of midgut sections dissected at 24 h PBM from *desat1*-silenced females at 18 h PE revealed failure to form the PM, allowing direct contact of bacterial cells with EC microvilli. Midgut architecture apparently remained intact (Fig. 1h). This observation suggests that in the absence of a PM, bacteria or other pathogens may be able to invade the hemocoel, potentially threatening mosquito survival.

To determine whether gut bacterial overgrowth is responsible for the observed mortality, we administered antibiotics via sugar meals after adult emergence to eliminate most gut microbiota. Notably, even under axenic conditions, 18 h PE *desat1*-silenced females died shortly after blood feeding, resembling the mortality observed in non-axenic counterparts (Supplementary Fig. 5a). In contrast, mosquitoes that were silenced at 72 h PE did not exhibit blood–feeding-induced mortality, regardless of antibiotic treatment (Supplementary Fig. 5b). These results suggest that gut bacterial over-proliferation is not a cause of the lethal outcome following blood feeding.

Silencing *desat1* disrupts lipid metabolism of newly emerged females

Mosquito TAG is primarily stored in the fat body as energy reserves[24]. Using Oil Red O staining, we observed that TAG is present in the fat body of females at 24 h PE and gradually accumulated at later time points (Supplementary Fig. 6a). Colorimetric measurements confirmed this trend: TAG content was low at 12–18 h PE and increased by 72 h PE (Supplementary Fig. 6b). Although blood meal digestion is energy-demanding and typically results in reduction of TAG content in *Aedes aegypti*[12,24], we did not detect a significant decrease in *An. stephensi* TAG content following a blood meal (Supplementary Fig. 6b).

Silencing *desat1* in newly emerged females significantly reduced TAG accumulation (Fig. 2a). At 18 h PE, TAG content of *desat1*-silenced females was markedly lower than that of the ds*GFP*-treated controls, regardless of whether mosquitoes received a sugar or a blood meal (Fig. 2a, b). In contrast, silencing *desat1* at 72 h PE had no effect on TAG

https://doi.org/10.1038/s41467-025-65407-6

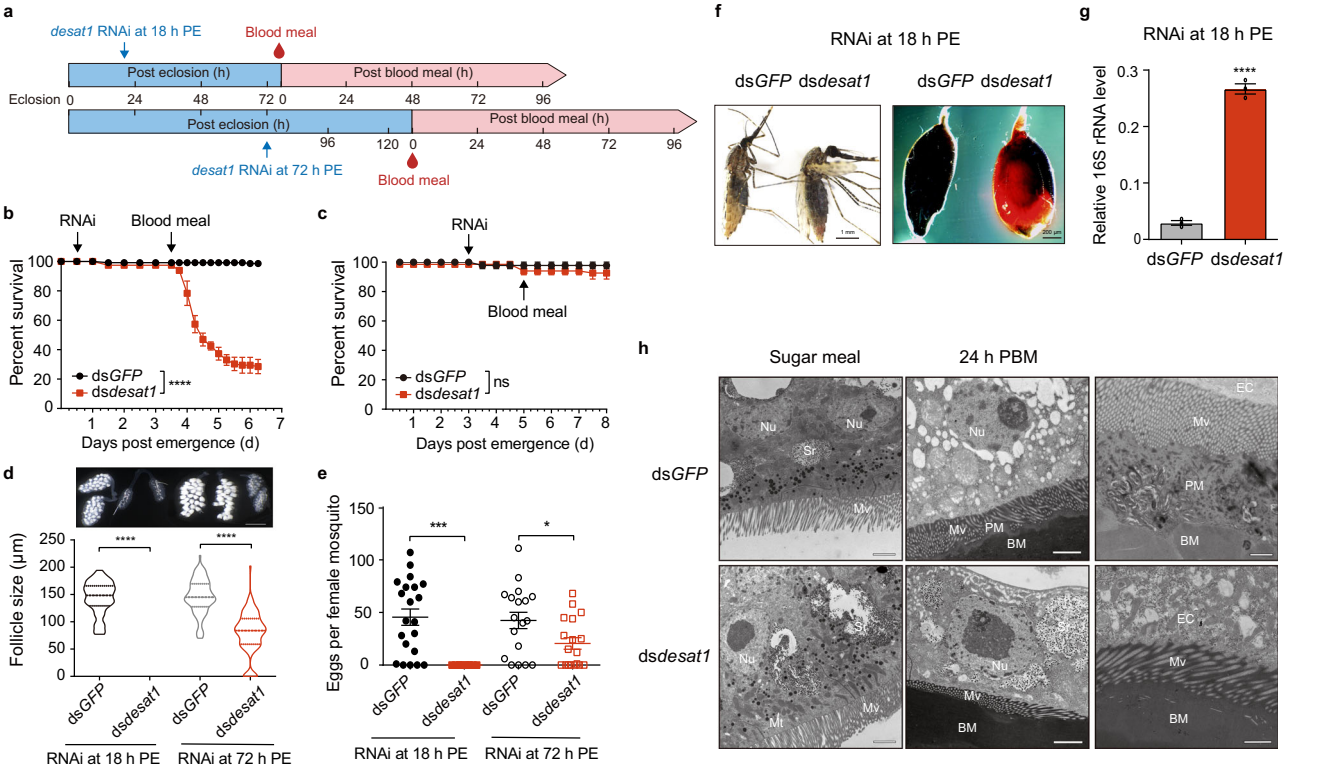

Fig. 1 | *desat1* knockdown of newly-emerged female mosquitoes leads to blood-induced lethality, reduced fecundity, and absence of the peritrophic matrix. **a** Schematic of the experimental design. Female mosquitoes were injected with ds*desat1* or ds*GFP* (control) at either 18 h or 72 h post-eclosion (PE). After a 3-day recovery period, a blood meal was provided and mosquito survival was recorded. Pre- and post-blood-feeding survival of female mosquitoes injected with ds*desat1* or ds*GFP* at 18 h PE (**b**) and 72 h PE (**c**) ($n = 40$). Statistics were performed using the Log-rank (Mantel-Cox) test. Similar results were obtained from three biological repeats. **d** Average ovarian follicle size of females injected with ds*desat1* or ds*GFP* at different PE times. Ovaries from surviving females were dissected at 24 h post-blood meal (PBM), and lengths of 6 ovarian follicles per female were measured ($n = 15$). The follicles of female mosquitoes injected with ds*desat1* at 18 h PE underwent complete developmental arrest and were recorded as 0 μm. Similar results were obtained from two biological repeats. Violin plots display the full distribution: center line: median; upper/lower hinges: 75th and 25th percentiles. **e** Egg numbers per female at 3d PBM, comparing ds*desat1*- and ds*GFP*-treated individuals at different PE stages ($n = 18$). Similar results were obtained from two biological repeats. **f** Representative images of whole mosquitoes and dissected midguts at 24 h PBM from females injected with ds*GFP* or ds*desat1* at 18 h PE. **g** Quantification of total midgut bacteria at 24 h PBM in mosquitoes injected with ds*desat1* at 18 h PE (see panel a). **h** Transmission electron microscope (TEM) images of midguts dissected from sugar-fed mosquitoes and at 24 h PBM following ds*GFP* or ds*desat1*injection at 18 h PE. Scale bars on the left and center panels = 2 μm; the right panel shows an enlarged view of the center images with scale bars = 1 μm. EC, epithelial cell; Mv, microvilli; PM, peritrophic matrix; BM, blood meal; Nu, nucleus; Sr, storage reservoir with several granules; Mt, mitochondrion. All error bars represent SEM. In **d** and **g**, statistics were performed with Student's *t* test. In **e**, significant difference was analyzed using the Mann-Whitney test. *, $p < 0.05$; ***, $p < 0.001$, ****, $p < 0.0001$. Source data are provided as a Source Data file.

content (Fig. 2a, b), indicating that the TAG reserves are established during early post-eclosion.

To further characterize lipid metabolic content of *desat1*-silenced mosquitoes, we performed liquid chromatography-mass spectrometry (LC-MS) of newly emerged females (18 h PE). There was a substantial reduction of glycerolipid content, including TAG and diacylglycerol (DAG), following either sugar or blood feeding compared to ds*GFP* controls (Fig. 2c and Supplementary Data 1). In contrast, the glycerophospholipid contents [including phosphatidylcholine (PC), phosphatidylethanolamine (PE), and phosphatidylglycerol (PG)] and sphingolipids [such as ceramide (Cer) and sphingomyelin (SM)] were significantly elevated (false discovery rate [FDR] <0.05) (Fig. 2c). These results indicate that *desat1* silencing of newly emerged females profoundly alters lipid composition. However, no significant changes were observed in overall lipid composition when *desat1* was silenced at 72 h PE (Fig. 2c).

Desat1 is a key enzyme involved in the conversion of saturated fatty acids (SFAs) to unsaturated fatty acids (USFAs)[16], and thus, the USFA/SFA ratio serves as a reliable indicator of Desat1 activity. At 18 h PE, silencing of *desat1* led to a marked decrease in the USFA/SFA ratio compared to ds*GFP* controls (Fig. 2d). Notably, when focusing on long-chain fatty acids (C16 and C18), which are primary substrates of Desat1[16], we observed a significant increase of stearic acid (C18:0) and a pronounced decrease of oleic acid (C18:1) in both sugar-fed and blood-fed mosquitoes (Fig. 2e, f). Additionally, palmitoleic acid (C16:1) abundance was also significantly reduced, yet we did not observe the expected increase of palmitic acid (C16:0) in 18 h PE *desat1*-silenced mosquitoes (Fig. 2e, f), suggesting that other metabolic pathways might influence palmitic acid turnover. In contrast, silencing *desat1* at 72 h PE did not impact TAG content (Fig. 2a, b) or overall lipid composition (Fig. 2c), although the USFA/SFA ratio was still significantly lower compared to ds*GFP* controls following either a sugar or blood meal (Fig. 2g). Under these conditions, the content of C16:0 and C18:0 was elevated, while C16:1 and C18:1 abundance remained unchanged (Fig. 2h, i).

Collectively, these results underscore the critical role of *desat1* in maintaining lipid homeostasis, particularly at early post-eclosion times. Early silencing of *desat1* profoundly perturbs lipid composition, reducing glycerolipid synthesis while promoting the accumulation of glycerophospholipids and sphingomyelin. In contrast, silencing *desat1* in mature adults (i.e., 72 h PE) lowers the USFA/SFA ratio, but overall lipid composition remains relatively stable.

https://doi.org/10.1038/s41467-025-65407-6

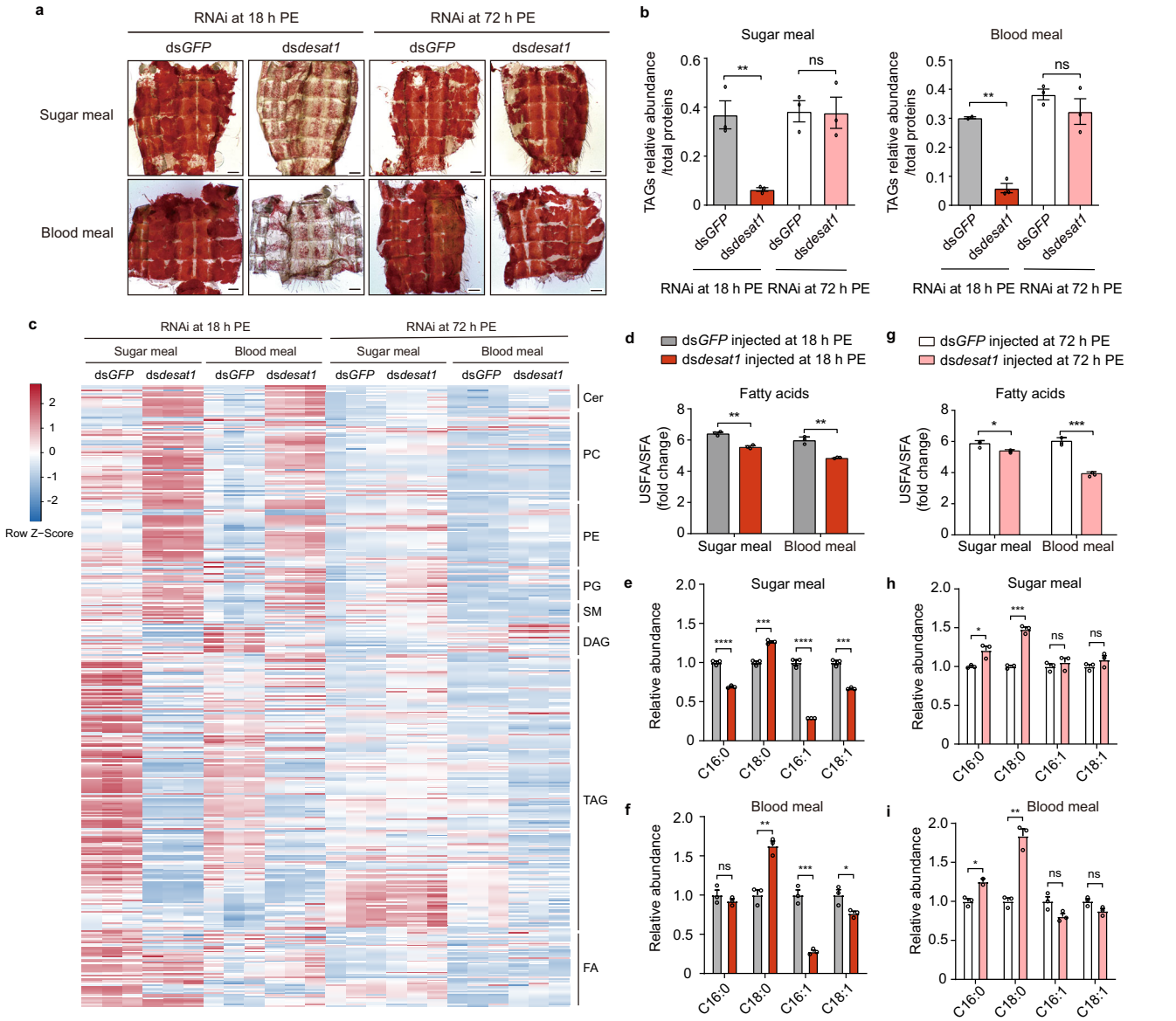

Fig. 2 | *desat1* silencing significantly alters lipid composition of newly emerged female mosquitoes. a Oil Red O-stained fat bodies of sugar- or blood-fed females injected with ds*GFP* or ds*desat1* at 18 h or at 72 h PE. **b** Relative triacylglycerol (TAG) abundance of fat bodies of sugar- or blood-fed females injected with ds*GFP* or ds*desat1* at 18 h or 72 h PE. TAG measurements were normalized to the total proteins. Similar results were obtained from three biological repeats. **c** Heatmap of lipid classes of *desat1*-silenced mosquitoes before and after a blood meal. Female mosquitoes were injected with *dsdesat1* or *dsGFP* (control) at either 18 h or 72 h PE. After a 3-day recovery, lipid was extracted before and after a blood meal (24 h PBM). Each column represents an independent sample ($n = 3$), and each row corresponds to a specific lipid type: Cer: ceramide; PC: phosphatidylcholine; PE: phosphatidylethanolamine; PG: phosphatidylglycerol; SM: sphingomyelin; DAG: diacylglycerol; TAG: triacylglycerol; FA: fatty acid. **d** Ratio of unsaturated to saturated fatty acids (USFA/SFA) of 18 h PE *desat1*-silenced mosquitoes pre- and post-blood meal (24 h PBM). Relative abundance of major saturated and unsaturated fatty acids of 18 h PE *desat1*-silenced mosquitoes fed with sugar (**e**) or blood (**f**). C16:0: palmitic acid; C16:1: palmitoleic acid; C18:0: stearic acid; C18:1: oleic acid. **g** USFA/SFA ratio in 72 h PE *desat1*-silenced mosquitoes before and after a blood meal (24 h PBM). Relative abundance of major saturated and unsaturated fatty acids of 72 h PE *desat1*-silenced mosquitoes fed with sugar (**h**) or blood (**i**). *Desat1*-RNAi treatments were normalized to *GFP*-RNAi treatments. Error bars indicate SEM. Statistics were performed with Student's *t*-test. *, $p < 0.05$; **, $p < 0.01$; ***, $p < 0.001$; ****, $p < 0.0001$. Source data are provided as a Source Data file.

Silencing *desat1* results in ROS stress and apoptosis following a blood meal, which can be mitigated by palmitoleic acid or oleic acid supplementation

In mammals, elevated free fatty acid content enhances both mitochondrial and peroxisomal metabolism, leading to increased production of reactive oxygen species (ROS)[25]. To determine whether ROS are induced in mosquitoes whose *desat1* gene is silenced at 18 h PE, we measured the expression of five ROS-related genes in the fat body. In mosquitoes maintained on sugar diet, *desat1* silencing resulted in no significant changes in the transcript abundance of *dual oxidase* (*Duox*), *NADPH oxidase 5* (*Nox5*), and *heme peroxidase 2* (*Hpx2*) genes (Fig. 3a). Following a blood meal, there was a marked upregulation of *Duox*, *Nox5*, *Hpx2*, and *nitric oxide synthase* (*Nos*) genes (Fig. 3a). Furthermore, *catalase*, a key antioxidant enzyme gene, was upregulated in *desat1*-silenced mosquitoes after a blood meal (Fig. 3a), leading to an increase in hydrogen peroxide (H_2O_2) content (Fig. 3b). These results suggest that silencing *desat1* at an early stage after eclosion triggers substantial ROS generation following a blood meal.

Excess SFAs often cause lipotoxicity when deposited in non-adipose tissues, leading to cell dysfunction or cell death in hepatocyte

https://doi.org/10.1038/s41467-025-65407-6

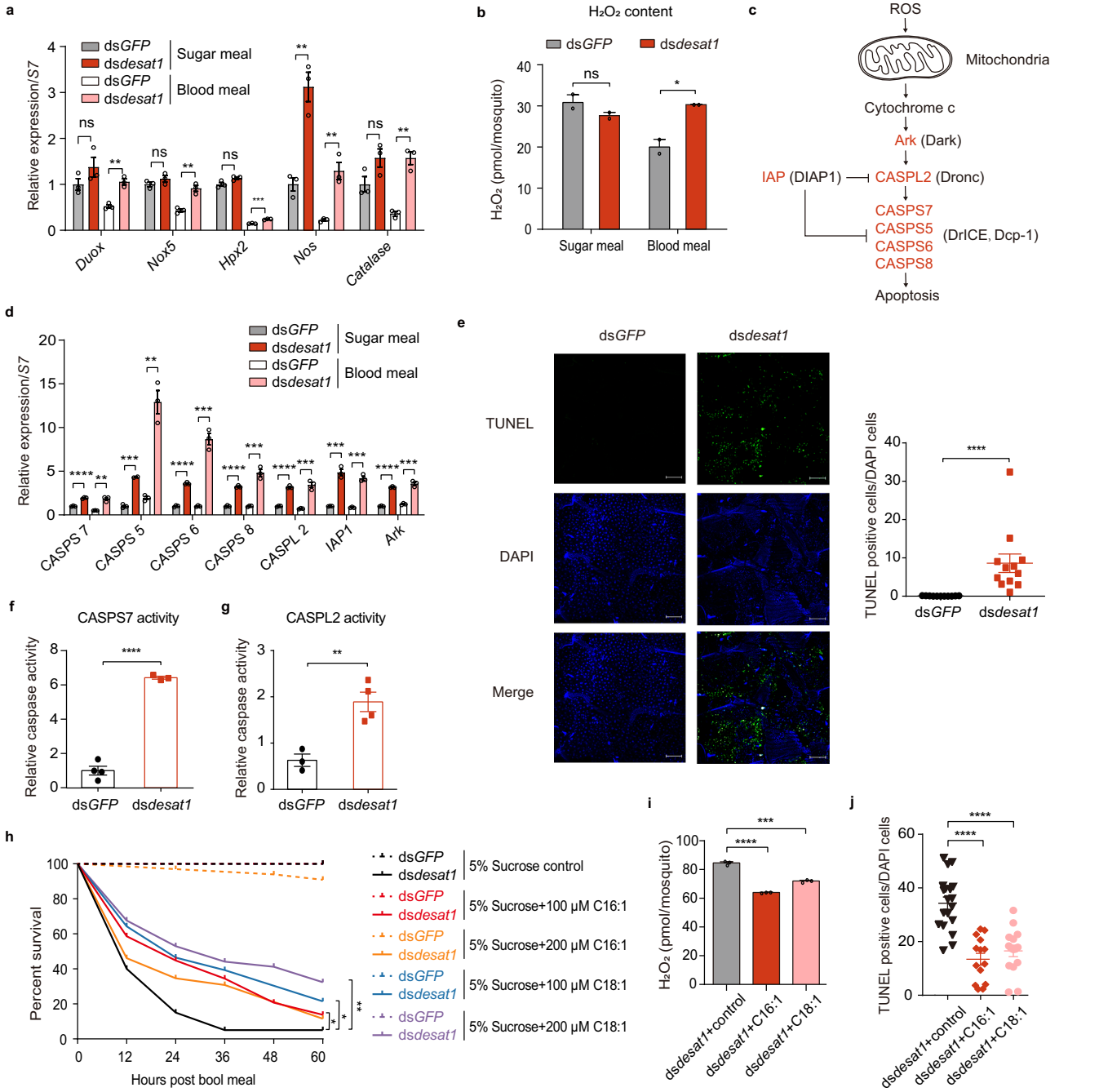

Fig. 3 | Silencing *desat1* of newly-emerged female mosquitoes induces ROS production and cell apoptosis. a Relative expression of ROS-related genes in *desat1*-silenced female mosquitoes fed with a sugar or blood meal (12 h PBM). **b** Hydrogen peroxide (H_2O_2) content of *desat1*-silenced female mosquitoes that were provided sugar only or a blood meal (12 h PBM) ($n = 20$). **c** Schematic diagram of the inferred apoptotic pathway in *An. stephensi* (red text), with *D. melanogaster* as a reference (gene names in parentheses)[81]. **d** Relative expression of apoptosis-related genes in *desat1*-silenced female mosquitoes fed sugar only or a blood meal (12 h PBM). **e** TUNEL staining of fat bodies from *desat1*-silenced females at 12 h PBM ($n = 15$). The proportion of TUNEL-positive cells relative to DAPI-stained cells was quantified. The scale bar is 200 μm. The horizontal lines in the graph represent medians, with error bars indicating the SEM. Significance was determined using the Mann-Whitney test. CASPS7 (**f**) and CASPL2 (**g**) activity in fat bodies of ds*desat1*- and ds*GFP*-injected females at 12 h PBM ($n = 30$). **h** Post-blood-meal survival of *desat1*-silenced females supplemented with palmitoleic acid (C16:1) or oleic acid (C18:1) ($n = 30$). Statistics were performed using the Log-rank (Mantel-Cox) test. **i** H_2O_2 content of *desat1*-silenced females supplemented with 200 μM palmitoleic acid (C16:1) or oleic acid (C18:1), measured at 12 h PBM ($n = 20$). An equivalent volume of ethanol as USFA stock solution was used as a control. **j** Proportion of TUNEL-positive cells at 12 h PBM in fat bodies of *desat1*-silenced females supplemented with 200 μM palmitoleic acid (C16:1) or oleic acid (C18:1) ($n = 15$). The horizontal lines represent medians, and error bars indicate SEM. Significance was determined using the Mann-Whitney test. Unless noted otherwise, female mosquitoes were injected with *dsdesat1* or *dsGFP* (control) at 18 h PE and were analyzed after a 3-day recovery. Statistical significance was performed using Student's *t*-test. *, $p < 0.05$; **, $p < 0.01$; ***, $p < 0.001$; ****, $p < 0.0001$. All experiments were repeated at least two times with similar results. Source data are provided as a Source Data file.

https://doi.org/10.1038/s41467-025-65407-6

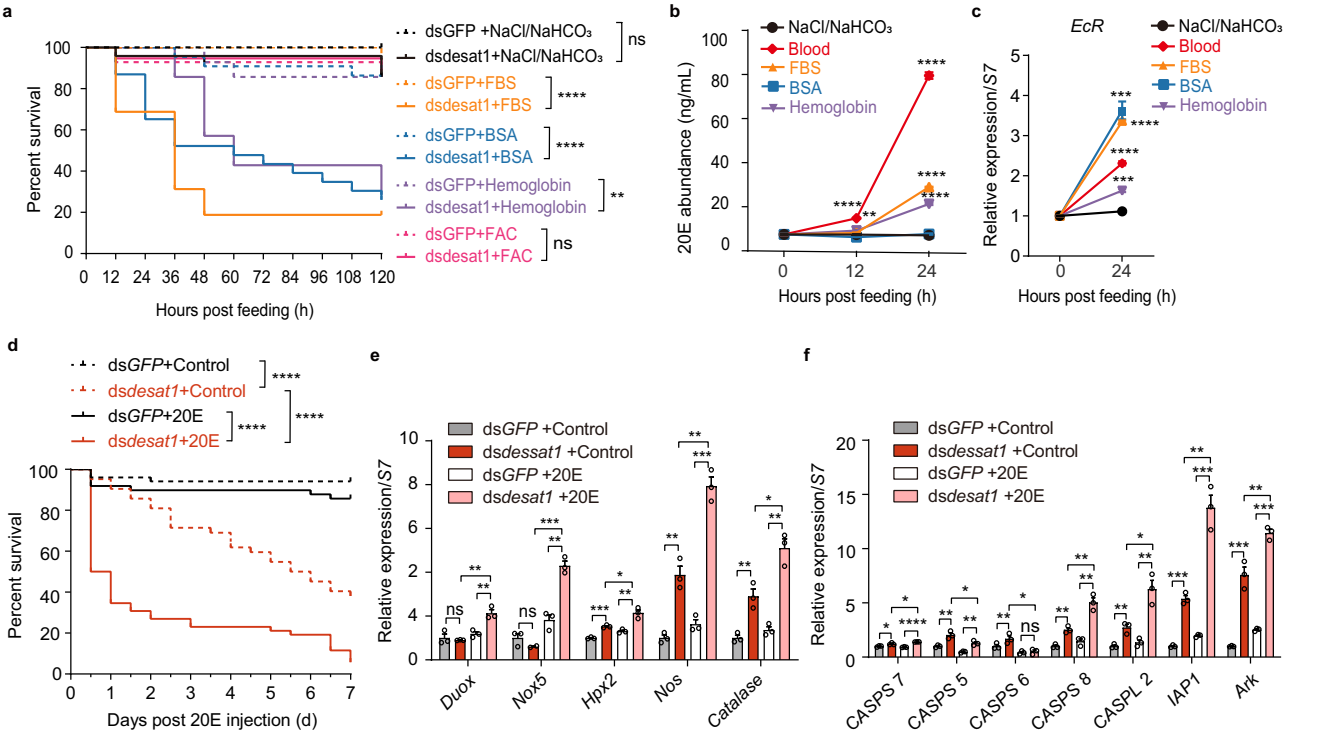

Fig. 4 | Host blood proteins induce mortality in early *desat1*-silenced female mosquitoes by activating the 20E pathway. a Survival of 18 h PE *desat1*-silenced females after feeding on different blood components ($n = 20$). FBS: fetal bovine serum; BSA: bovine serum albumin; FAC: ferric ammonium citrate. **b** Quantification of 20E in females at 12 h and 24 h after feeding on blood components, as determined by UHPLC-MS/MS ($n = 30$). **c** qPCR analysis of 20E receptor gene *EcR* expression at 24 h after feeding on blood components. Mosquitoes fed with NaCl/$NaHCO_3$ solution served as controls for each time point. **d** Survival of 18 h PE *desat1*-silenced females injected with a 20E solution. Mosquitoes injected with ethanol solution served as controls ($n = 40$). **e** qPCR analysis of ROS-related gene expression and **f** apoptosis-related gene expression in early *desat1*-silenced females injected with 1 mM 20E solution. Error bars represent SEM. In **a** and **d**, statistics were performed using the Log-rank (Mantel-Cox) test. In **b** and **c**, statistical analysis was performed with multiple t-test, with correction for multiple comparisons using the Holm-Šídák method. In the remaining panels, statistics were performed with Student's *t*-test. *, $p < 0.05$; **, $p < 0.01$; ***, $p < 0.001$; ****, $p < 0.0001$. All experiments were repeated at least two times with similar results. Source data are provided as a Source Data file.

and cardiomyocyte cell lines[25,26]. We hypothesized that the dysregulated lipid metabolism and increased ROS production resulting from *desat1* silencing of newly emerged mosquitoes would induce programmed cell death. Apoptosis in *Anopheles* mosquitoes involves a proteolytic cascade of cysteinyl aspartate-specific proteinases belonging to the caspase family[27,28]. By comparing the *D. melanogaster* and *An. gambiae* genomes, we identified homologous *An. stephensi* caspase genes (Supplementary Fig. 7). Based on their prodomain sequences, these caspases are classified as the initiator caspase CASPL2 and the effector caspases CASPS5, CASPS6, CASPS7, and CASPS8 (Fig. 3c). In the fat body of *desat1*-silenced mosquitoes, the expression of these major apoptosis-related genes was significantly higher than in ds*GFP* controls, regardless of whether the mosquitoes were fed sugar or blood (Fig. 3d). Terminal deoxynucleotidyl transferase-mediated dUTP nick end labeling (TUNEL) assay revealed a higher proportion of apoptotic cells in the fat body (Fig. 3e), accompanied by elevated activities of initiator CASPL2 and effector CASPS7 following a blood meal (Fig. 3f, g). Taken together, these data suggest that a blood meal triggers lipotoxicity and increased ROS production in early *desat1*-silenced mosquitoes, resulting in cellular damage and apoptosis—factors that likely contribute to mosquito mortality.

We observed a pronounced reduction of USFAs, specifically palmitoleic acid (C16:1) and oleic acid (C18:1), in 18 h PE *desat1*-silenced mosquitoes (Fig. 2e, f). Moreover, USFA supplementation has been shown to mitigate apoptosis[29,30]. Accordingly, we supplemented newly emerged *desat1*-silenced females with 100 µM or 200 µM C16:1 or C18:1 via sugar meals for 3 days. As expected, survival after a blood meal was significantly improved with supplementation of these USFAs (Fig. 3h), with C18:1 exerting a stronger, dose-dependent protective effect compared to C16:1 (Fig. 3h). Supplementation of C16:1 or C18:1 also significantly reduced ROS production (Fig. 3i) and decreased apoptosis (Fig. 3j and Supplementary Fig. 8). These results highlight the protective role of C16:1 and C18:1 against blood meal-induced oxidative stress and cell apoptosis in *desat1*-silenced females.

Host blood proteins activate the 20E pathway, exacerbating oxidative stress and apoptosis in early *desat1*-silenced females

To identify the blood-meal component responsible for the mortality of early *desat1*-silenced females, we fed mosquitoes with different blood-derived components, supplemented with ATP as a phagostimulant[31]. Feeding with fetal bovine serum (FBS), bovine serum albumin (BSA), or hemoglobin led to rapid mortality (Fig. 4a). While toxic by-products of blood digestion, such as heme and iron, are known to be harmful to mosquitoes[11], feeding ferric ammonium citrate (FAC)—an iron source analogous to heme[32,33]—did not affect the survival of *desat1*-silenced females (Fig. 4a). These results indicate that protein components in the blood meal, rather than iron alone, are responsible for inducing mortality in females in which *desat1* is silenced at the newly emerged stage.

In female mosquitoes, blood ingestion triggers the synthesis of 20-hydroxyecdysone (20E)[34], a pivotal regulator of lipid metabolism[24,35]. To pinpoint the blood components driving this response, we quantified 20E by LC–MS/MS after feeding mosquitoes defined components of blood. Hemoglobin and whole blood significantly increased 20E titer at 12 h post-feeding, whereas FBS elicited a noticeable increase at 24 h post-feeding (Fig. 4b). By contrast, BSA did not elevate 20E levels at either 12 h or 24 h post-feeding (Fig. 4b).

https://doi.org/10.1038/s41467-025-65407-6

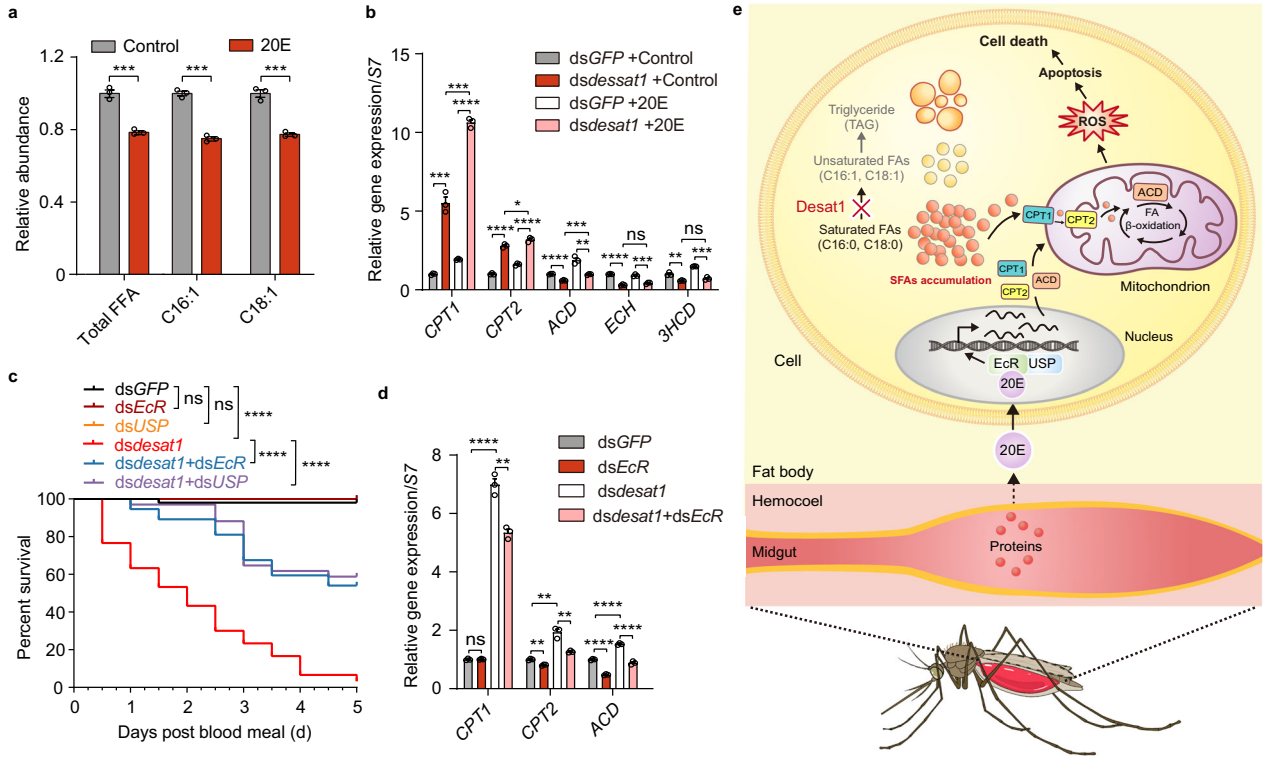

Fig. 5 | 20E promotes fatty acid oxidation in early *desat1*-silenced female mosquitoes. a Total fatty acids, palmitoleic acid (C16:1), and oleic acid (C18:1) content in the fat body of adult female mosquitoes at 24 h post−20E injection. Fatty acid content was measured using UPLC-MS/MS (3 independent repeats per group). **b** Expression of five key genes involved in fatty acid oxidation (*CPT1*, *CPT2*, *ACD*, *ECH*, and *3HCD*) in early *desat1*-silenced mosquitoes at 24 h post-20E injection. **c** Post-blood-meal survival of 18 h PE *desat1*-silenced females with *EcR* or *USP* knockdown ($n = 40$). Statistics were performed using the Log-rank (Mantel-Cox) test. **d** Relative expression of key genes involved in fatty acid oxidation in *desat1*- and *EcR*-silenced mosquitoes at 12 h PBM. Error bars represent SEM. In **a**, **b** and **d**, statistics were performed with Student's *t* test. *, $p < 0.05$; **, $p < 0.01$; ***, $p < 0.001$; ****, $p < 0.0001$. All experiments were repeated at least two times with similar results. **e** A model illustrating how loss of *desat1* function disrupts lipid metabolism and leads to lethality following a blood meal. Silencing *desat1* in newly emerged female mosquitoes impairs the conversion of SFAs to USFAs, thereby reducing triglyceride synthesis. The resulting decrease in USFA/SFA ratio leads to the accumulation of SFAs, triggering oxidative stress and cell apoptosis. Mechanistically, following a blood meal, proteins in the ingested blood stimulate 20E synthesis and activate the 20E signaling pathway, further enhancing fatty acid β-oxidation, increasing ROS production, and inducing apoptosis in the *desat1*-silenced early-emerged female mosquitoes, ultimately leading to mosquito death. Source data are provided as a Source Data file.

However, all these components upregulated the expression of the ecdysone receptor gene, *EcR* (Fig. 4c).

Injection of 20E into early *desat1*-silenced females led to a significant increase in mortality (Fig. 4d), likely by promoting the expression of genes associated with ROS generation in the *desat1*-silenced mosquitoes (Fig. 4e). Additionally, genes involved in apoptosis were upregulated by 20E (Fig. 4f). Taken together, these results indicate that elevated 20E content enhances oxidative stress and cell apoptosis in early *desat1*-silenced mosquitoes, ultimately leading to mortality.

20E promotes an increase of fatty acid oxidation after a blood meal in early *desat1*-silenced females

Fatty acids are metabolized in mitochondria and peroxisomes through β-oxidation, a process that generates ROS[36,37]. Following injection of 20E into early *desat1*-silenced mosquitoes, we observed a reduction of fat body free fatty acids, particularly C16:1 and C18:1 (Fig. 5a and Supplementary Data 2). Previous studies have shown that 20E accelerates β-oxidation of fatty acids and promotes lipolysis[24,38]. The transport of fatty acyl-CoA into mitochondria, regulated by carnitine palmitoyltransferase-1 (CPT1) and CPT2, represents a rate-limiting step in fatty acid β-oxidation[39]. We found that expression levels of *CPT1* and *CPT2* were significantly higher in *desat1*-silenced mosquitoes than in ds*GFP* controls (Fig. 5b). Furthermore, the genes encoding CPT1, CPT2, and acyl-CoA dehydrogenase (ACD) —the first enzyme of the β-oxidation cycle, were all upregulated by 20E (Fig. 5b).

20E function is mediated through its nuclear receptor complex, composed of the EcR and ultraspiracle (USP)[40,41]. To investigate the role of this pathway, we utilized RNAi to knock down *EcR* or *USP* in both ds*GFP* controls and early *desat1*-silenced females (Supplementary Fig. 9). Knockdown of *EcR* or *USP* expression had no impact on the survival of ds*GFP*-treated control mosquitoes but substantially reduced mortality of early *desat1*-silenced females following a blood meal (Fig. 5c). Consistently, knockdown of *EcR* in early *desat1*-silenced mosquitoes led to a marked reduction in *CPT1*, *CPT2*, and *ACD* expression (Fig. 5d). These results indicate that inhibition of the 20E signaling pathway in *desat1*-silenced mosquitoes mitigates the lethal effect driven by excessive 20E-activated fatty acid β-oxidation.

Discussion

Previous studies on insect *desaturase* genes have primarily focused on their role in synthesizing cuticular hydrocarbons[18,42,43]. Our previous study also demonstrated that *desat1* regulates the synthesis of the sex pheromone heptacosane in male *Anopheles* mosquitoes[19]. In this study, by silencing *desat1* in female *An. stephensi*, we discovered a crucial function of *desat1* during early adult stages: the maintenance of lipid homeostasis to ensure survival and successful reproduction following a blood meal (Fig. 5e). These findings expand the current understanding of *desat1* function and highlight its developmental and physiological significance in lipid metabolism, extending our knowledge beyond its previously characterized roles in hydrocarbon and pheromone biosynthesis.

Desaturase catalyzes the production of unsaturated fatty acids, a process that is both crucial and evolutionarily conserved across mammals and insects[44]. In mice and fruit flies, knocking out this gene reduces lipogenesis and promotes lipolysis, leading to body fat loss and delayed development[17,45–47]. Loss of *desat1* function also significantly shortens the lifespan of insects[21,22], with particularly pronounced effects observed in female mosquitoes following blood feeding[48]. To assess the functional conservation of *desat1* across mosquito species, we identified its homolog (*AAEL003203*) in *Ae. aegypti* by comparative genomic analysis. Silencing of *Ae. aegypti desat1* recapitulated the lethal phenotype observed in *An. stephensi*, causing a significant increase in post-blood-meal mortality ($p < 0.0001$ vs. ds*GFP* controls) (Supplementary Fig. 10). Protein sequence alignment revealed > 82% identity among mosquito species, with strict conservation of catalytic residues critical for Δ9-desaturase activity. These findings indicate that *desat1* plays an evolutionarily conserved role in lipid metabolism, representing a cross-species metabolic vulnerability that could be exploited for targeted vector control.

Our study provides mechanistic insights relating to the post-blood-meal mortality of *desat1*-silenced mosquitoes. We show that proper *desat1* function within the first 24 h post-eclosion is essential for converting SFAs into USFAs and production of TAG. Disruption of *desat1* during this narrow window results in an accumulation of SFAs that trigger lipotoxicity, manifested as elevated ROS production via fatty acid oxidation in mitochondria, ultimately leading to cell apoptosis[25,49,50]. These findings highlight how ROS generation and apoptotic cell death lead to reduced mosquito lifespan. Unlike newly emerged females, mature mosquitoes (i.e., 72 h PE) with established lipid reserves are more resilient to *desat1* knockdown, exhibiting only moderate changes in UFA/SFA ratio without destabilizing overall lipid homeostasis. This minimal metabolic perturbation accounts for the absence of post-blood-meal mortality in older mosquitoes, which display normal survival rates. These findings highlight the temporal specificity of desat1 function, with its critical role confined primarily to the early phase of lipid reserve establishment.

Previous studies in various model systems have shown that excess long-chain SFAs (e.g., C16:0 and C18:0) lead to lipotoxicity[51,52]. Conversely, supplementing cells with USFAs or activating the *SCD1* gene (the mammalian homolog of insect *desat1*) can rescue lipotoxicity-induced cell damage[25,51,53]. In this study, supplementation of *desat1*-silenced mosquitoes with C16:1 or C18:1 rescued mortality, indicating that C16:0 and C18:0 are the main long-chain SFAs driving lipotoxicity in mosquitoes. *Desat1* knockdown led to a more pronounced reduction in C16:1 than in C18:1, indicating that *desat1* may preferentially catalyze C16:1 synthesis in mosquitoes. However, dietary supplementation with C16:1 alone may not be sufficient to fully restore its physiological functions, particularly in mitigating blood meal-induced mortality. These observations suggest that while C18:1 confers broader survival benefits, C16:1 likely fulfills more specialized roles in antioxidant defense that cannot be completely compensated by exogenous supplementation.

Fatty acids are fundamental building blocks for various lipids[54]. Both glycerolipids and glycerophospholipids are synthesized de novo by incorporating fatty acids into a glycerol backbone[55–57]. In newly emerged female *Anopheles*, *desat1* silencing impairs SFA-to-USFA conversion, disrupting TAG synthesis and storage while increasing glycerophospholipid and sphingolipid abundance. In mammalian cardiomyocytes, excess fatty acids are redirected into phospholipid biosynthesis once they exceed the cell's metabolic capacity[58]. Phospholipids, as the primary components of cell membranes, determine membrane fluidity and homeostasis[59]. Imbalances of phospholipid composition can affect multiple cellular processes, including signal transduction, cell growth, membrane trafficking, and apoptosis[60–62]. Moreover, studies in mammals have shown that excess free fatty acids resulting from *SCD1* deficiency can be diverted into the de novo ceramide synthesis pathway[63,64], ultimately inducing cell apoptosis[65]. Therefore, the loss of cell membrane integrity and apoptosis associated with abnormal phospholipid and ceramide content may contribute to the mortality of *desat1*-silenced mosquitoes.

In mosquitoes, the blood meal-induced steroid hormone 20E integrates nutritional cues to regulate reproduction and lipid metabolism[1,24,66]. Among the blood proteins tested, most of them stimulate 20E synthesis and activate the 20E pathway, except for BSA. Interestingly, a previous study in *An. darlingi* found that BSA feeding did not support normal egg production or larval hatching[67]. However, studies in *Aedes* mosquitoes reported that BSA can stimulate ecdysteroid production and support normal egg laying[68,69].This discrepancy suggests that *Aedes* and *Anopheles* mosquitoes may differ in their energy demands for reproduction, and that BSA alone may be insufficient to trigger 20E synthesis in *Anopheles* mosquitoes.

The hormone 20E has been shown to accelerate fatty acid β-oxidation in various insects[24,38]. In blood-feeding female *Ae. aegypti*, the 20E/EcR complex regulates the transcription of hepatocyte nuclear factor 4 (HNF4), which directly binds to the promoter of lipid metabolism genes (e.g., genes encoding very long chain acyl-CoA dehydrogenase and 3-ketoacyl-CoA thiolase), thereby activating fatty acid β-oxidation and accelerating lipolysis[24]. In *desat1*-silenced *An. stephensi* females, excessive fatty acid β-oxidation triggers ROS production and apoptosis, directly leading to mortality. However, when the 20E pathway is blocked via *EcR* or *USP* knockdown, the expression of key β-oxidation genes is suppressed, thus decreasing post-blood-meal mortality. This finding suggests that 20E likely regulates lipid metabolism genes in *An. stephensi* via EcR-mediated signal transduction. Interestingly, knockdown of *desat1* in mature female mosquitoes (72 h post-eclosion) neither impairs post-blood-meal survival nor disrupts TAG accumulation, although it reduces the USFA/SFA ratio and inhibits reproduction. Notably, *desat1* expression and TAG content are very low in newly emerged mosquitoes, gradually increasing with age, facilitating the conversion of SFAs to USFAs and promoting TAG storage. Thus, knocking down *desat1* early on (within 24 h of emergence) critically disrupts lipid synthesis, whereas later knockdown does not affect existing lipid stores or composition. Although the USFA fraction is reduced in *desat1*-silenced mature females, they retain enough stored lipids to meet 20E-driven metabolic demands post-blood feeding, thereby avoiding mortality. Nevertheless, these nutrient constraints still adversely affect oogenesis, leading to diminished fecundity.

Additionally, we observed that silencing *desat1* in newly emerged females affects midgut peritrophic matrix (PM) formation, potentially contributing to mortality after blood feeding. Chitin, a key PM component, is synthesized by glucosamine:fructose-6-phosphate amidotransferase (Gfat) and chitin synthase (CHS)[70,71]. However, in previous studies, interfering with the expression of these genes prevents PM formation yet does not kill female mosquitoes after blood feeding[70]. Our data demonstrate that axenic mosquitoes lacking gut microbiota still exhibit mortality following *desat1* knockdown (Supplementary Fig. 5), indicating that although PM deficiency facilitates direct bacterial contact with the midgut epithelium, this structural defect is not the primary cause of post-blood-meal lethality. In *D. melanogaster* and *An. coluzzii*, previous studies also found that *desat1*-deficient flies exhibit smaller midguts[25], and its knockdown in *An. coluzzii* affects midgut physiology and membrane integrity[48]. These results suggest that *desat1* deficiency in early emerged mosquitoes may also impair early midgut development and cellular function.

In conclusion, this study underscores the pivotal role of *desat1* in safeguarding female mosquitoes against 20E-induced lipotoxicity and establishes a metabolic fail-safe mechanism that ensures survival in blood-feeding insects. By linking a classical lipid metabolic enzyme to steroid hormone signaling and organismal survival, our work uncovers a critical regulatory axis and identifies *desat1* as a promising target for

genetic or RNAi-based mosquito control. Given that effective suppression of *desat1* appears to require a relatively narrow time window, its translational potential will hinge on the development of rapid and efficient delivery strategies.

Methods

Mosquito rearing

Anopheles stephensi (Dutch strain) mosquitoes were reared at 27 °C, 80% ± 5% relative humidity (RH) under a 12 h light/12 h dark cycle. Adult mosquitoes were maintained on 10% (w/v) sucrose solution after eclosion and the larvae were fed with cat food pellets and ground fish food supplement.

RNA isolation, cDNA synthesis, and qPCR analysis

Total RNA was isolated from *An. stephensi* using RNAiso Plus (9109, TaKaRa, Dalian, China) according to the manufacturer's instructions. cDNA was synthesized using the PrimeScript™ RT Reagent Kit with genomic DNA removal (RR047, TaKaRa, Dalian, China), following the manufacturer's instructions. Gene expression was assessed by quantitative real-time PCR (qPCR) using the Thermo PikoReal 96 (Thermo Fisher Scientific) with AceQ® qPCR SYBR® Green Mix Master (Q111, Vazyme, Nanjing, China). The qPCR reaction consisted of an initial denaturation at 95 °C for 5 minutes, followed by 40 cycles of 10 seconds at 94 °C and 30 seconds at 60 °C, and a final extension at 60 °C for 30 seconds before deriving a melting curve (60–95 °C). To quantify gut bacterial load, genomic DNA was isolated from mosquito midguts and subjected to qPCR with bacterium-specific primers to amplify 16S ribosomal RNA (rRNA) fragments. The *An. stephensi* housekeeping gene *RPS7* (*AsS7*) was used as an internal control. Primer sequences are listed in the Supplementary Table 1.

dsRNA-mediated gene silencing in mosquitoes

Double-stranded RNAs (dsRNAs) targeting *desat1* (ds*desat1*), *EcR* (ds*EcR*), and *USP* (ds*USP*) were synthesized by first amplifying the respective coding regions from *An. stephensi* cDNA using forward and reverse primers containing the T7 promoter sequence (TAATACGACTCACTATAGGG) at their 5′ ends (see Supplementary Table 1). The dsRNA was then synthesized using the MEGAscript RNAi kit (AM1626, Invitrogen, Carlsbad, CA, USA) and purified with the accompanying column. Enhanced Green Fluorescent Protein gene dsRNA (ds*GFP*) was synthesized as a negative control. For dsRNA microinjection, cold-anesthetized female mosquitoes were injected with 138 nl of dsRNA solution (1.5 μg/μl) into the hemocoel using a Nanoject II microinjector (Drummond). To simultaneously interfere with the expression of two genes, ds*desat1* and the other dsRNA (ds*EcR* or ds*USP*) were mixed to an equal final concentration of 1.5 μg/μl, and then injected into newly emerged female mosquitoes. The injected mosquitoes were allowed to recover for 2-3 days before further experiments.

Survival rate assay

Newly or lately emerged female mosquitoes were injected with dsRNA, with each group consisting of at least 30 mosquitoes and three replicates. The mosquitoes injected with ds*GFP* served as a control. On day 3 post-injection, the mosquitoes were starved for 10 h and then allowed to feed on anesthetized mice for 15 min. Fully engorged mosquitoes were selected for survival rate assays, and mortality was recorded every 6 h or 12 h post a blood meal (PBM). To assess the impact of gut microbiota on survival, mosquitoes were treated with antibiotic solutions as described previously[72] to eliminate the gut bacteria. Newly emerged ds*desat1*-treated female mosquitoes were supplied with 5% sucrose containing 100 μg/mL penicillin, 10 μg/mL streptomycin, 25 μg/mL gentamicin, and 100 μg/mL kanamycin for 3 days. Subsequently, the mosquitoes were fed with a blood meal, and mortality was recorded post-blood feeding.

Female mosquito fertility assay

To assess oocyte development, ovaries were dissected from females at 24 h PBM in phosphate-buffered saline (PBS) and photographed under an Olympus stereomicroscope ($n = 15$ mosquitoes per group). Lengths of ovarian follicles were measured along the anterior-posterior axis using ImageJ software. Six ovarian follicles were randomly selected from a pair of ovaries for each mosquito, and their average length was calculated using ImageJ software. For egg-laying assessment, female mosquitoes were individually separated to lay eggs in 2 mL tubes containing moistened filter paper inside the cap at 3 d PBM, and placed in a dark box at a 27 °C incubator for 24 h. The number of eggs laid by each female was counted under a stereomicroscope.

Preparation and examination of histological sections

Histological sections from blood-fed mosquito midguts were prepared as previously described[73,74]. In brief, abdomens were dissected from female mosquitoes at 24 h PBM and fixed in 2.5% glutaraldehyde at 4 °C. The samples were dehydrated in a series of acetone (30–100%) and embedded in Epoxy resin. Ultra-thin sections (approximately 100 nm) were stained and observed under a Hitachi H-7700 transmission electron microscope (TEM).

Trypsin activity assay

Trypsin activity of the female mosquito midgut was analyzed according to a previously described protocol[75]. Midguts from ds*desat1*- and ds*GFP*-injected mosquitoes were dissected at 12 h PBM in cold PBS (4 °C) and washed to remove blood meal residues. Twenty midguts from each group were individually homogenized in 100 μL Tris-HCl buffer (50 mM Tris-HCl, 10 mM $CaCl_2$, pH 8.0). For each sample, 20 μL of homogenate supernatants were added to 160 μL 1 mM Nα-benzoyl-DL-arginine-p-nitroanilide (BAPNA) (B4875, Sigma). The absorbance was measured at 405 nm with a microplate reader (Thermo Fisher Scientific) before and after a 10-minute reaction (ΔA405nm). The calculation formula is as follows: Trypsin activity (unit) = (ΔA405nm × dilution factor) / (volume of sample/ mL).

Qualitative and quantitative determination of TAG

Lipid in the fat bodies of female mosquitoes was visualized by Oil Red O staining. Mosquitoes were dissected and fixed in 4% paraformaldehyde solution (dissolved in 1× PBS with 0.1% Triton X-100) at 4 °C for 2 h. After washing three times with 1× PBS, the samples were stained by the Oil Red O Staining Kit (C0157, Beyotime Biotech, Shanghai, China) according to the manufacturer's instructions, and then observed under an Olympus MVX10 stereomicroscope. TAG is quantitatively measured with the GPO-PAP Triglyceride Assay Kit (S0219, Beyotime Biotech, Shanghai, China) according to the manufacturer's instructions. Fat bodies of 20 female mosquitoes dissected from each group were homogenized in 200 μL of lysis buffer. The supernatant was collected for reaction with the kit reagents, and the absorbance was assayed using a microplate reader (Thermo Fisher Scientific) with a wavelength of 570 nm. Protein concentration was determined using Pierce™ BCA Protein Assay Kit (23227, Thermofisher, Waltham, MA, USA) according to the manufacturer's instructions.

Lipid extraction and lipidome analysis by UPLC-MS/MS

Total lipids were extracted from ds*desat1*- and ds*GFP*-injected mosquitoes following established protocols[76,77]. Briefly, 30 mosquitoes were homogenized together in 700 μL of H_2O in conical glass centrifuge tubes, and 2.1 mL CH_2Cl_2/MeOH (1:2, v/v) was added to each sample. After thoroughly vortexing and incubation for 1 h, 700 μL H_2O and 700 μL CH_2Cl_2 were added, and the mixture was inverted and mixed several times to facilitate phase separation. After centrifugation, the lower organic layer was collected and concentrated under nitrogen flow. Each sample was dissolved in 50 μL of a solvent mixture

containing CH_2Cl_2/IPA/ACN/H_2O (20:65:35:5, v/v/v/v). Lipidomic analyses were performed on Q Exactive quadrupole-Orbitrap high-resolution mass spectrometry coupled with a Dionex Ultimate 3000 RSLC (HPG) ultra-performance liquid chromatography (UPLC-Q-Orbitrap-HRMS) system (Thermo Fisher Scientific), with a heated electrospray ionization (HESI) source. Two microliters of each sample were injected onto an Acclaim C30 column (2.1 mm × 150 mm, 3 µm; Thermo Fisher Scientific) under the following liquid chromatography conditions: mobile phase A (acetonitrile: water, 60:40, v/v, containing 2 mM ammonium formate) and mobile phase B (isopropanol: acetonitrile, 90:10, v/v, containing 2 mM ammonium formate). The gradient of B was as follows: 0.0 min, 30.0%; 2.1 min, 55.0%; 12.0 min, 65%; 18.0 min, 85.0%; 20.0 min, 100.0%; 25.0 min, 100.0%; 25.1 min, 30.0%; 28.0 min, 30.0%. The flow rate was 0.26 mL/min at 50 °C. MS experiments were performed in positive and negative ion modes using a heated ESI source. The source and ion transfer parameters applied were as follows: spray voltage 3.5 kV (positive) / 2.8 kV (negative). For the ionization mode, the sheath gas, aux gas, capillary temperature and heater temperature were maintained at 40, 10 (arbitrary units), 275 °C and 350 °C, respectively. The S-Lens RF level was set at 50. The Orbitrap mass analyzer was operated at a resolving power of 70,000 in full-scan mode (scan range: 200-1800 m/z; automatic gain control (AGC) target: 1e6) and of 17,500 in the Top 10 data-dependent MS2 mode (lipid inclusion list on; stepped normalized collision energy: 20 and 35; injection time: 80 ms; isolation window: 1.5 m/z; AGC target: 1e5) with a dynamic exclusion setting of 6.0 seconds. Lipidomic data were collected using Xcalibur Software (v4.2.47, Thermo Fisher Scientific) and processed using MS-DIAL (version 4.7.0). Raw files were converted to.*abf* format and imported with MS1 and MS2 tolerances of 0.005 Da and 0.01 Da, respectively. Feature extraction used a peak height threshold of 1000, mass slice width 0.1 Da, and RT alignment tolerance 0.05 min. Lipid identifications were assigned against LipidBlast, requiring MS/MS similarity scores >80% with fragment ion tolerance of 0.05 Da. Adducts considered included $[M+H]^+$, $[M+Na]^+$, $[M+NH4]^+$, $[M-H]^-$, and [M + HCOO]. The processed data was further analyzed with Heatmapper (http://www.heatmapper.ca/) for visualizing clustering of data.

Measurement of hydrogen peroxide production

The production of hydrogen peroxide (H_2O_2) was determined using the Hydrogen Peroxide Assay Kit (S0038, Beyotime Biotech, Shanghai, China) following the manufacturer's protocol. The assay is based on the reaction where H_2O_2 oxidizes Fe^{2+} to Fe^{3+}. The Fe^{3+} ions then form a complex with xylenol orange dye to yield a purple product that exhibits maximum absorbance at 560 nm. Midguts and fat body from 20 mosquitoes per sample were homogenized in 200 µL of lysis buffer and centrifuged to obtain the supernatant. 50 µL of the supernatants were mixed with 100 µL of test solutions from the Hydrogen Peroxide Assay Kit and then incubated at room temperature for 20 min. The absorbance was measured immediately at 560 nm using a spectrophotometer. The concentration of H_2O_2 released was calculated from a hydrogen peroxide standard curve. Each measurement was repeated three times.

TUNEL staining for cell apoptosis

Mosquito abdomens were dissected in 1× PBS buffer, and the epidermis was cut along the anterior-posterior axis. The samples were then fixed in 4% paraformaldehyde solution (dissolved in 1× PBS) for 30 min at room temperature. The fat bodies attached to the epidermis were stained for apoptosis and cell nuclei using the TUNEL Bright-Green Apoptosis Detection Kit (A112, Vazyme, Nanjing, China) and DAPI Nuclear Staining Dye (C1005, Beyotime Biotech, Shanghai, China), respectively, according to the manufacturer's protocols. TUNEL-labeled green fluorescence and DAPI-stained blue fluorescence were visualized using a ZEISS LSM880 laser confocal microscope.

Caspase activity assay

In *An. stephensi*, CASPL2 is an initiator caspase protein homologous to Dronc in *Drosophila melanogaster*, whereas CASPS7 is an effector caspase protein homologous to Drice in *D. melanogaster*. Initiator caspases cleave substrates such as LEHD, and effector caspases cleave substrates such as DEVD[78,79]. To assess caspase activity, the activities of CASPS7 and CASPL2 were measured using the chromogenic substrates Ac-DEVD-*p*NA (P9710, Beyotime Biotech, Shanghai, China) and Ac-LEHD-*p*NA (P9728, Beyotime Biotech, Shanghai, China), respectively. Newly emerged female mosquitoes were injected with ds*desat1* or ds*GFP* at 18 h PE and were fed blood after a 3-day recovery period. At 12 h PBM, fat bodies from 30 mosquitoes were dissected in 1× PBS buffer and homogenized in 200 µL lysis buffer. The samples were incubated on ice for 5 min, followed by centrifugation. The supernatants were then reacted with 2 mM Ac-DEVD-*p*NA and 2 mM Ac-LEHD-*p*NA substrate as per the manufacturer's instructions to measure the activities of CASPS7 and CASPL2, respectively. Absorbance was measured at 405 nm with a microplate reader (Thermo Fisher Scientific). Protein concentration was determined using Pierce™ BCA Protein Assay Kit (23227, Thermofisher, Waltham, MA, USA) according to the manufacturer's instructions. The *p*NA product levels in the samples were quantified using standard curves for *p*NA. Caspase activity was defined as the amount of *p*NA released per microgram of sample protein per minute.

Palmitoleic acid and oleic acid treatment

Palmitoleic acid (C16:1) and oleic acid (C18:1) (Sigma, Catalog numbers 76169 and 75090, respectively) were prepared as 100 mM stock solutions by dissolving in 100% ethanol and stored at −20 °C. The stock solutions were subsequently diluted into a 5% sucrose solution to achieve final concentrations of 100 µM or 200 µM. Newly emerged female *An. stephensi* mosquitoes, injected with ds*desat1* or ds*GFP* at 18 h PE, were fed with 100 µM or 200 µM palmitoleic acid or oleic acid solutions. As a control, a 5% sucrose solution containing an equivalent volume of ethanol as the unsaturated fatty acid stock solution was fed to ds*desat1*- and ds*GFP*-treated mosquitoes. The mosquitoes were allowed to feed on palmitoleic acid or oleic acid for 3 d before proceeding with further experiments.

Mosquito feeding with different blood components

To examine the effects of different blood components on mosquito survival, ds*desat1*- and ds*GFP*-treated female mosquitoes were fed with 200 mg/mL bovine serum albumin (BSA) (A23088, Abcone, Beijing, China), 20 mg/mL hemoglobin (H828504, Macklin, Shanghai, China), fetal bovine serum (FBS) (10099141 C, Gibco, Victoria, Australia), or 5 mM ferric ammonium citrate (FAC). BSA, hemoglobin, and FAC were diluted in a NaCl/$NaHCO_3$ solution (110 mM NaCl, 20 mM $NaHCO_3$), which was fed to mosquitoes as the negative control. Mouse blood was used as the positive control. ATP was added to a final concentration of 1 mM in all the blood components as a phagostimulant to trigger engorgement[31]. Various blood components were filtered through 0.22 µm filters (SLGPR33RB, Merck) and fed to mosquitoes, which had been starved for 10 h, using membrane feeders. Fully engorged mosquitoes were selected for survival rate assays or measurement of 20-hydroxyecdysone (20E) concentration.

Measurement of 20E concentration by UHPLC-MS/MS

Mosquito samples for 20E measurement by UHPLC-MS/MS were prepared according to the methods described by Duo Peng et al.[80]. Whole bodies from 30 female mosquitoes were homogenized in 500 µL of 100% methanol at 12 h and 24 h after feeding on blood and various blood components. After homogenization with a bead beater, 500 µL of 100% methanol was added to the sample, which was then incubated on ice for 20 min. The supernatants were collected following centrifugation at 12,000 × *g* for 5 min. The pellet underwent a second

methanol extraction using 500 µL of 100% methanol. The supernatants from both extractions were combined and dried under nitrogen flow. The dried extract was resuspended in 100 µL of 80% methanol in water. The samples were analyzed using QTRAP 6500+ mass spectrometer (AB Sciex) equipped with an electrospray ionization (ESI) source (AB Sciex), coupled with a UHPLC instrument ExionLC 30 AD (AB Sciex) with ACQUITY UPLC® BEH C18 (1.7 µm, 2.1 × 50 mm, Waters™) set at 40 °C column temperature and flow rate of 0.3 mL/min. The injection volume was 1 µL. The liquid chromatography conditions were mobile phase A (water, containing 0.1% formic acid) and mobile phase B (ACN, containing 0.1% formic acid). The LC gradient program was as follows: 0.5 min at 5% B; increasing to 50% B in 4.5 min; further increasing to 99% B in 0.5 min; followed by 1.5 min at 99% B; and re-equilibrated at 5% B for 3 min. Ionization in the MS source was heated electrospray ionization in positive mode: ion spray voltage, 5.5 kV; ion spray temperature, 500 °C; curtain gas, 35 psi; ion source gas 1, 50 psi; ion source gas 2, 50 psi. The mass spectrometer measured data in multiple reaction monitoring (MRM) mode. The 20E standard (H811106, Macklin, Shanghai, China) was diluted with 80% methanol in a gradient concentration of 200, 100, 20, 10, 2, and 1 ng/mL for standard curves. Fresh standards were prepared daily. Calibration curves were obtained by plotting concentration versus peak area using $1/x^2$ weighting. The correlation coefficient (r) of each curve exceeds 0.99. Data were extracted using Analyst 1.6.3 software (AB Sciex) and quantified using MultiQuant 3.0.2 software (AB Sciex). 20E quantification was based on the comparison of the peak area to standard curves, calculating the absolute amounts in each sample. This experiment was repeated twice.

Preparation of 20E solution and mosquito treatment

The insect steroid hormone 20E (H811106, Macklin, Shanghai, China) was dissolved in 100% ethanol to prepare a 20 mM stock solution, which was stored at −20 °C. The stock solutions were further diluted with 1× PBS buffer to 1 mM for mosquito injection. Newly emerged female mosquitoes were injected with ds*desat1* or ds*GFP* at 18 h PE, with 30 mosquitoes in each group. After a 3-day recovery period, these mosquitoes were injected with 50 nL of 1 mM 20E solution by Nanoject II microinjector (Drummond). Control mosquitoes were injected with PBS buffer containing the same volume of ethanol as the 20E stock solution. The survival rate was recorded every 12 h after injection. The gene expression was analyzed at 24 h post-20E injection. The experiments were repeated three times.

Multiple sequence alignment of desat1 orthologs

Multiple sequence alignment of desat1 orthologs was performed using DNAMAN 9.0.1 to assess evolutionary conservation across mosquito species. Full-length protein sequences from *Drosophila melanogaster* (CG5887), *Anopheles gambiae* (AGAP001713), *Anopheles stephensi* (ASTE006887), *Anopheles arabiensis* (AARA21_008839), *Anopheles coluzzii* (ACON2_037373), *Anopheles darlingi* (ADAR2_001713), *Anopheles sinensis* (ASIC013829), *Aedes aegypti* (AAEL003203), *Aedes albopictus* (AALFPA_043344), and *Culex quinquefasciatus* (CQUJHB007391) were aligned using global alignment mode with the BLOSUM62 substitution matrix, gap opening penalty of 10, and a gap extension penalty of 1. Conserved domains corresponding to the OLE1 fatty acid desaturase superfamily (COG1398) were manually verified against the NCBI Conserved Domain Database. Sequence identities were calculated using the built-in similarity index of DNAMAN.

Statistical analysis

The statistical significance of the survival data was analyzed with a log-rank (Mantel–Cox) test. The statistical significance of multiple group comparisons was analyzed using a one-way ANOVA test. Tukey's HSD tests were applied as follow-up analyses only when the ANOVA reached statistical significance ($p < 0.05$). The statistical significance of egg numbers was analyzed using a two-tailed Mann–Whitney test. Other comparisons were calculated using a two-tailed Student's *t*-test for unpaired comparisons between two groups. A value of $p < 0.05$ was considered statistically significant. All statistical analyses were performed using GraphPad Prism software for Windows. Lipidomic data were normalized to total lipid content. Individual lipid species were analyzed using a univariate model, and *p*-values were adjusted for multiple testing using the Benjamini–Hochberg false discovery rate (FDR) method. Lipids with FDR < 0.05 were considered statistically significant.

Reporting summary

Further information on research design is available in the Nature Portfolio Reporting Summary linked to this article.

Data availability

The data supporting the findings of this study are available in the article and the Supplementary Materials. Mass spectrometry lipidomics data provided in the Supplementary Data and the raw data are available on the MetaboLights repository under accession code MTBLS12928. Source data are provided with this paper.

References

1. Roy, S., Saha, T. T., Zou, Z. & Raikhel, A. S. Regulatory pathways controlling female insect reproduction. *Annu Rev. Entomol.* **63**, 489–511 (2018).
2. dos Santos Aguilar, J. G. An overview of lipids from insects. *Biocatal. Agric Biotechnol.* **33**, 101967 (2021).
3. Arrese, E. L. & Soulages, J. L. Insect fat body: energy, metabolism, and regulation. *Annu Rev. Entomol.* **55**, 207–225 (2010).
4. Downer, R. G. H. & Matthews, J. R. Patterns of lipid distribution and utilisation in insects. *Am. Zool.* **16**, 733–745 (1976).
5. Gondim, K. C., Atella, G. C., Pontes, E. G. & Majerowicz, D. Lipid metabolism in insect disease vectors. *Insect Biochem Mol. Biol.* **101**, 108–123 (2018).
6. Barillas-Mury, C., Ribeiro, J. M. C. & Valenzuela, J. G. Understanding pathogen survival and transmission by arthropod vectors to prevent human disease. *Science* **377**, eabc2757 (2022).
7. WHO. Global vector control response 2017-2030. World Health Organization, Geneva (2017).
8. WHO. World Malaria Report 2023. World Health Organization, Geneva (2023).
9. Barredo, E. & DeGennaro, M. Not just from blood: mosquito nutrient acquisition from nectar sources. *Trends Parasitol.* **36**, 473–484 (2020).
10. Briegel, H. Physiological bases of mosquito ecology. *J. Vector Ecol.* **28**, 1–11 (2003).
11. Nouzova, M., Clifton, M. E. & Noriega, F. G. Mosquito adaptations to hematophagia impact pathogen transmission. *Curr. Opin. Insect Sci.* **34**, 21–26 (2019).
12. Hou, Y. et al. Temporal coordination of carbohydrate metabolism during mosquito reproduction. *Plos Genet.* **11**, e1005309 (2015).
13. Kikuchi, K. & Tsukamoto, H. Stearoyl-CoA desaturase and tumorigenesis. *Chem-Biol. Interact.* **316**, 108917 (2020).
14. Heier, C. & Kuhnlein, R. P. Triacylglycerol metabolism in *Drosophila melanogaster*. *Genetics* **210**, 1163–1184 (2018).
15. Ravaut, G., Legiot, A., Bergeron, K. F. & Mounier, C. Monounsaturated fatty acids in obesity-related inflammation. *Int. J. Mol. Sci.* **22**, 330 (2021).
16. Nagao, K., Murakami, A. & Umeda, M. Structure and function of Δ9-fatty acid desaturase. *Chem. Pharm. Bull.* **67**, 327–332 (2019).
17. Ntambi, J. M. et al. Loss of stearoyl-CoA desaturase-1 function protects mice against adiposity. *Proc. Natl. Acad. Sci. USA* **99**, 11482–11486 (2002).

18. Dallerac, R. et al. A Δ9 desaturase gene with a different substrate specificity is responsible for the cuticular diene hydrocarbon polymorphism in *Drosophila melanogaster*. *Proc. Natl. Acad. Sci. USA* **97**, 9449–9454 (2000).
19. Wang, G. D. et al. Clock genes and environmental cues coordinate *Anopheles* pheromone synthesis, swarming, and mating. *Science* **371**, 411–415 (2021).
20. Liu, S. et al. *Clock* genes regulate mating activity rhythms in the vector mosquitoes, *Aedes albopictus* and *Culex quinquefasciatus*. *PLoS Negl. Trop. Dis*. **16**, e0010965 (2022).
21. Joseph, N. M., Elphick, N. Y., Mohammad, S. & Bauer, J. H. Altered pheromone biosynthesis is associated with sex-specific changes in life span and behavior in *Drosophila melanogaster*. *Mech. Ageing Dev.* **176**, 1–8 (2018).
22. Zeng, J. M., Ye, W. F., Noman, A., Machado, R. A. R. & Lou, Y. G. The Desaturase gene family is crucially required for fatty acid metabolism and survival of the brown planthopper, *Nilaparvata lugens*. *Int. J. Mol. Sci.* **20**, 1369 (2019).
23. Erlandson, M. A., Toprak, U. & Hegedus, D. D. Role of the peritrophic matrix in insect-pathogen interactions. *J. Insect Physiol.* **117**, 103894 (2019).
24. Wang, X. et al. Hormone and receptor interplay in the regulation of mosquito lipid metabolism. *P Natl. Acad. Sci. USA* **114**, E2709–E2718 (2017).
25. Tuthill li, B. F., Quaglia, C. J., O'Hara, E. & Musselman, L. P. Loss of Stearoyl-CoA desaturase 1 leads to cardiac dysfunction and lipotoxicity. *J. Exp. Biol*. **224**, jeb240432 (2021).
26. Yazici, D. & Sezer, H. Insulin resistance, obesity and lipotoxicity. *Adv. Exp. Med Biol.* **960**, 277–304 (2017).
27. Danial, N. N. & Korsmeyer, S. J. Cell death: critical control points. *Cell* **116**, 205–219 (2004).
28. Kumar, S. & Dorstyn, L. Analysing caspase activation and caspase activity in apoptotic cells. *Methods Mol. Biol.* **559**, 3–17 (2009).
29. Urso, C. J. & Zhou, H. Palmitic acid lipotoxicity in microglia cells is ameliorated by unsaturated fatty acids. *Int. J. Mol. Sci.* **22**, 9093 (2021).
30. Chen, X. et al. Oleic acid protects saturated fatty acid mediated lipotoxicity in hepatocytes and rat of non-alcoholic steatohepatitis. *Life Sci.* **203**, 291–304 (2018).
31. Jove, V. et al. Sensory discrimination of blood and floral nectar by *Aedes aegypti* mosquitoes. *Neuron* **108**, 1163–1180.e1112 (2020).
32. Duchemin, J. B. & Paradkar, P. N. Iron availability affects West Nile virus infection in its mosquito vector. *Virol J.* **14**, 103 (2017).
33. Marro, S. et al. Heme controls ferroportin1 (FPN1) transcription involving Bach1, Nrf2 and a MARE/ARE sequence motif at position-7007 of the FPN1 promoter. *Haematologica* **95**, 1261–1268 (2010).
34. Dhara, A. et al. Ovary ecdysteroidogenic hormone functions independently of the insulin receptor in the yellow fever mosquito. *Insect Biochem Mol. Biol.* **43**, 1100–1108 (2013).
35. Ling, L. & Raikhel, A. S. Cross-talk of insulin-like peptides, juvenile hormone, and 20-hydroxyecdysone in regulation of metabolism in the mosquito *Aedes aegypti*. *Proc. Natl Acad. Sci. USA* **118**, e2023470118 (2021).
36. Holmström, K. M. & Finkel, T. Cellular mechanisms and physiological consequences of redox-dependent signalling. *Nat. Rev. Mol. Cell Biol.* **15**, 411–421 (2014).
37. Ma, Y. B. et al. Fatty acid oxidation: An emerging facet of metabolic transformation in cancer. *Cancer Lett.* **435**, 92–100 (2018).
38. Zhang, S. Y. et al. Steroid hormone 20-hydroxyecdysone disturbs fat body lipid metabolism and negatively regulates gluconeogenesis in *Hyphantria cunea* larvae. *Insect Sci.* **30**, 771–788 (2023).
39. Kastaniotis, A. J. et al. Mitochondrial fatty acid synthesis, fatty acids and mitochondrial physiology. *Mol. Cell Biol. L* **1862**, 39–48 (2017).
40. Yao, T. P. et al. Functional ecdysone receptor is the product of *EcR* and *ultraspiracle* genes. *Nature* **366**, 476–479 (1993).
41. Thomas, H. E., Stunnenberg, H. G. & Stewart, A. F. Heterodimerization of the *Drosophila* ecdysone receptor with retinoid X receptor and ultraspiracle. *Nature* **362**, 471–475 (1993).
42. Grigoraki, L., Grau-Bové, X., Yates, H. C., Lycett, G. J. & Ranson, H. Isolation and transcriptomic analysis of *Anopheles gambiae* oenocytes enables the delineation of hydrocarbon biosynthesis. *eLife* **9**, e58019 (2020).
43. Krupp, J. J. et al. Social experience modifies pheromone expression and mating behavior in male *Drosophila melanogaster*. *Curr. Biol.* **18**, 1373–1383 (2008).
44. Flowers, M. T. & Ntambi, J. M. Role of stearoyl-coenzyme A desaturase in regulating lipid metabolism. *Curr. Opin. Lipido* **19**, 248–256 (2008).
45. Musselman, L. P. et al. Role of fat body lipogenesis in protection against the effects of caloric overload in *Drosophila*. *J. Biol. Chem.* **288**, 8028–8042 (2013).
46. Parisi, F. et al. dMyc expression in the fat body affects DILP2 release and increases the expression of the fat desaturase Desat1 resulting in organismal growth. *Dev. Biol.* **379**, 64–75 (2013).
47. Wang, Y. W. et al. Inhibition of fatty acid desaturases in *Drosophila melanogaster* larvae blocks feeding and developmental progression. *Arch. Insect Biochem. Physiol.* **92**, 6–23 (2016).
48. Ferdous, Z. et al. *Anopheles coluzzii stearoyl*-CoA desaturase is essential for adult female survival and reproduction upon blood feeding. *PLoS Pathog.* **17**, e1009486 (2021).
49. Spalding, K. L. et al. Impact of fat mass and distribution on lipid turnover in human adipose tissue. *Nat. Commun.* **8**, 15253 (2017).
50. Hauck, A. K. & Bernlohr, D. A. Oxidative stress and lipotoxicity. *J. Lipid Res.* **57**, 1976–1986 (2016).
51. Listenberger, L. L., Ory, D. S. & Schaffer, J. E. Palmitate-induced apoptosis can occur through a ceramide-independent pathway. *J. Biol. Chem.* **276**, 14890–14895 (2001).
52. Maedler, K. et al. Distinct effects of saturated and monounsaturated fatty acids on β-cell turnover and function. *Diabetes* **50**, 69–76 (2001).
53. Eyme, K. M. et al. Targeting de novo lipid synthesis induces lipotoxicity and impairs DNA damage repair in glioblastoma mouse models. *Sci. Transl. Med.* **15**, eabq6288 (2023).
54. Jeon, Y. G., Kim, Y. Y., Lee, G. & Kim, J. B. Physiological and pathological roles of lipogenesis. *Nat. Metab.* **5**, 735–759 (2023).
55. Yamashita, A. et al. Glycerophosphate/acylglycerophosphate acyltransferases. *Biology* **3**, 801–830 (2014).
56. Dircks, L. & Sul, H. S. Acyltransferases of de novo glycerophospholipid biosynthesis. *Prog. Lipid Res.* **38**, 461–479 (1999).
57. Craven, P. A., Davidson, C. M. & DeRubertis, F. R. Increase in diacylglycerol mass in isolated glomeruli by glucose from de novo synthesis of glycerolipids. *Diabetes* **39**, 667–674 (1990).
58. de Vries, J. E. et al. Saturated but not mono-unsaturated fatty acids induce apoptotic cell death in neonatal rat ventricular myocytes. *J. Lipid Res.* **38**, 1384–1394 (1997).
59. Morita, S. Y. & Ikeda, Y. Regulation of membrane phospholipid biosynthesis in mammalian cells. *Biochem. Pharm.* **206**, 115296 (2022).
60. Wang, X., Devaiah, S. P., Zhang, W. & Welti, R. Signaling functions of phosphatidic acid. *Prog. Lipid Res.* **45**, 250–278 (2006).
61. Zhu, J., Wang, K. Z. & Chu, C. T. After the banquet: mitochondrial biogenesis, mitophagy, and cell survival. *Autophagy* **9**, 1663–1676 (2013).
62. Jenkins, G. M. & Frohman, M. A. Phospholipase D: a lipid centric review. *Cell. Mol. Life Sci.* **62**, 2305–2316 (2005).
63. Ji, C. Y. et al. Inhibition of ceramide de novo synthesis ameliorates meibomian gland dysfunction induced by SCD1 deficiency. *Ocul. Surf.* **22**, 230–241 (2021).
64. Sampath, H. et al. Skin-specific deletion of stearoyl-CoA desaturase-1 alters skin lipid composition and protects mice from high fat diet-induced obesity. *J. Biol. Chem.* **284**, 19961–19973 (2009).

65. Pettus, B. J., Chalfant, C. E. & Hannun, Y. A. Ceramide in apoptosis: an overview and current perspectives. *Mol. Cell Biol. L* **1585**, 114–125 (2002).
66. Hun, L. V. et al. Essential functions of mosquito ecdysone importers in development and reproduction. *Proc. Natl. Acad. Sci. USA* **119**, e2202932119 (2022).
67. da Silva Costa, G., Rodrigues, M. M. S. & Silva, A. A. E. Toward a blood-free diet for *Anopheles darlingi* (Diptera: Culicidae). *J. Med. Entomol.* **57**, 947–951 (2020).
68. Gonzales, K. K., Tsujimoto, H. & Hansen, I. A. Blood serum and BSA, but neither red blood cells nor hemoglobin can support vitellogenesis and egg production in the dengue vector *Aedes aegypti*. *Peerj* **3**, e938 (2015).
69. Pitts, R. J. A blood-free protein meal supporting oogenesis in the Asian tiger mosquito, *Aedes albopictus* (Skuse). *J. Insect Physiol.* **64**, 1–6 (2014).
70. Kato, N. et al. Regulatory mechanisms of chitin biosynthesis and roles of chitin in peritrophic matrix formation in the midgut of adult *Aedes aegypti*. *Insect Biochem Mol. Biol.* **36**, 1–9 (2006).
71. Lehane, M. J. Peritrophic matrix structure and function. *Annu Rev. Entomol.* **42**, 525–550 (1997).
72. Wei, G. et al. Insect pathogenic fungus interacts with the gut microbiota to accelerate mosquito mortality. *Proc. Natl. Acad. Sci. USA* **114**, 5994–5999 (2017).
73. Martins, G. F., Serrão, J. E., Ramalho-Ortigão, J. M. & Pimenta, P. F. Histochemical and ultrastructural studies of the mosquito *Aedes aegypti* fat body: effects of aging and diet type. *Microsc. Res. Tech.* **74**, 1032–1039 (2011).
74. Baton, L. A. & Ranford-Cartwright, L. C. *Plasmodium falciparum* ookinete invasion of the midgut epithelium of *Anopheles stephensi* is consistent with the Time Bomb model. *Parasitology* **129**, 663–676 (2004).
75. Isoe, J., Rascón, A. A. Jr., Kunz, S. & Miesfeld, R. L. Molecular genetic analysis of midgut serine proteases in *Aedes aegypti* mosquitoes. *Insect Biochem Mol. Biol.* **39**, 903–912 (2009).
76. Bligh, E. G. & Dyer, W. J. A rapid method of total lipid extraction and purification. *Can. J. Biochem. Physiol.* **37**, 911–917 (1959).
77. Guckert, J. B., Cooksey, K. E. & Jackson, L. L. Lipid sovent systems are not equivalent for analysis of lipid classes in the microeukaryotic green alga, *Chlorella*. *J. Microbiol. Methods* **8**, 139–149 (1988).
78. Crawford, E. D. & Wells, J. A. Caspase substrates and cellular remodeling. *Annu Rev. Biochem.* **80**, 1055–1087 (2011).
79. Talanian, R. V. et al. Substrate specificities of caspase family proteases. *J. Biol. Chem.* **272**, 9677–9682 (1997).
80. Peng, D. et al. A male steroid controls female sexual behaviour in the malaria mosquito. *Nature* **608**, 93–97 (2022).
81. Shi, Y. Caspase activation, inhibition, and reactivation: a mechanistic view. *Protein Sci.* **13**, 1979–1987 (2004).

Acknowledgements

This work was supported by the National Key R&D Program of China (2024YFA0917000 and 2023YFA1801000), the National Natural Science Foundation of China (grants 32021001, 32230015), the New Cornerstone Science Foundation (NCI202328), Shanghai Municipal Science and Technology Major Project, Three-Year Initiative Plan for Strengthening Public Health System Construction in Shanghai (2023–2025) Key Discipline Project (No. GWVI-11.1-12), and Chinese Academy of Science (317GJHZ2022028GC). We thank Professor Marcelo Jacobs-Lorena at Johns Hopkins Bloomberg School of Public Health for comments and proofreading the manuscript. We thank Xiaoyan Xu, Yuanyuan Gao, and Lianyan Jing from the Core Facility Centre, CAS Centre for Excellence in Molecular Plant Sciences, for assistance in liquid chromatography-mass spectrometry analysis and lipidome analysis, Xiaoyan Gao, Jiqin Li, Zhiping Zhang, and Lina Xu for technical support with electron microscopy, and Wenjuan Cai for technical support with confocal microscopy. We thank Gangqi Fang from the CAS Centre for Excellence in Molecular Plant Sciences for assisting with the statistical analysis of the lipidome.

Author contributions

S.W. conceived the project. S.W., P.S. and G.W. designed the study. P.S., G.W., C.C. and L.D. performed interference (RNAi) assays. P.S. and G.W. performed survival rate assays. P.S. and G.W. conducted TEM analysis. P.S., G.W., B.Y. and T.Z. conducted bioassays of trypsin activity, TAG content, and hydrogen peroxide production. P.S., Y.L. and T.Z. conducted TUNEL staining for cell apoptosis and caspase activity assay. P.S. and G.W. conducted lipidome analysis. P.S., G.W. and L.D. conducted 20E treatment and measurement of 20E concentration. P.S., G.W., F.L. and B.Y. reared mosquitoes. P.S., G.W. and S.W. analyzed the data. P.S., G.W., B.Y., Y.W. and S.W. wrote the manuscript.

Competing interests

The authors declare no competing interests.

Additional information

Supplementary information The online version contains supplementary material available at https://doi.org/10.1038/s41467-025-65407-6.

Correspondence and requests for materials should be addressed to Sibao Wang.

Peer review information *Nature Communications* thanks Paola Bellosta, Matthias Klein, and the other, anonymous reviewer(s) for their contribution to the peer review of this work. A peer review file is available.